Using Alpha Absorption to find the Thickness of Foils and the Specific Energy Loss of Alpha particles at different Air Pressures

Nikita Sichov - nsichov@ethz.ch
Supervisor: Dr. Lukas Wacker - wacker@phys.ethz.ch

December 10, 2025

Contents

Abstract

This experiment verifies theoretical conclusions on the behaviour of alpha particles when interacting with absorbers such as air, aluminium, and gold; additionally, it attempts to measure the distance dependent detection rate of an americium source in vacuum as well as the specific energy loss at different pressures. The results succesfully show a relation between two theoretical and computational approaches for finding the thickness of a foil of absorbers, with accuracies of about $\pm 10\%$. An example would be an aluminium foil with a width of $26.2 \pm 1.60 \mu m$. On the other hand, due to a misapproximation of the proper range for count change, we came to little conclusion in the question of count-distance relations. The pressure dependent energy loss has smooth behaviour and small errors, but stray from theoretical claims made towards straggling by Niels Bohr.

Introduction

Alpha particles consist of two protons and two neutrons bound together and are produced during alpha decay. This experiment observes interactions of the alpha decay of Americium:

$$^{241}\mathrm{Am} \longrightarrow ^{237}\mathrm{Np}^{*} + \alpha \tag{1}$$

Alpha decay is characterized as being highly ionizing with low penetration depth. These two attributes are the core drives of our scientific method in this report and they will be critically analysed and utilized [4].

Alpha particles interact with electrons and nuclei of target atoms by coulomb interaction, since these particles are ionized. Inelastic collision with electrons and elastic collision with nuclei both cause a loss in energy of the alpha particle. Considering a source and a target material, one can quantify these interactions and how the path of a alpha-ray is affected. One of these parameters is the *stopping power* which quantifies the mean energy loss per path length, then the *Bragg curve* characterizes the strong decrease of the stopping power near the end of the range.

Theoretical Background

Specific Energy Loss

We begin by considering the stray process of two particles. Particle 1 is defined with the mass and charge $(m_1, Z_1 e)$ and particle 2 with $(m_1, Z_1 e)$, we also have an impact parameter b as shown in Figure 1.

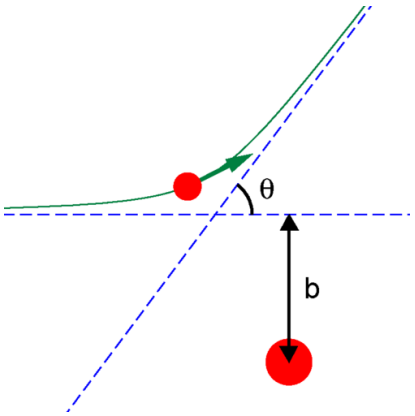

Figure 1: Collision diagram of particle 1 (small ball) and particle 2 (large ball).[5]

In this model, we know by conservation of momentum that the change in momentum and symmetry of the system that $\Delta p_x = 0$ disappears. For the y-direction we use coulomb's law and the divergence theorem to find that:

$$\Delta p_y = Z_1 e \int_{-\infty}^{\infty} F_y \, dt \approx \frac{Z_1 e}{2\pi b v} \frac{Q}{\varepsilon_0} = \frac{2 Z_1 Z_2}{bv} \epsilon^2$$

Where $\epsilon^2 := \frac{e^2}{4\pi\varepsilon_0}$. The resulting non-relativistic kinetic energy transfer ($T = \frac{(\Delta p)^2}{2m_2}$) is:

$$T = \frac{(\Delta p_{y,2})^2}{2m_2} = \frac{Z_1^2 Z_2^2 e^4}{b^2 E} \frac{m_1}{m_2} \tag{2}$$

We now generalize this process to more target particles, as in a medium. We say that it has an atomic density of N particles per volume and an atomic number Z (electrons per atom). Therefore, $n = NZ$ is the electrons per unit volume. The differential cross-section $d\sigma(T)$ for an energy transfer between dT is defined as $d\sigma(T) = -2\pi b db$.
Now we have to define and integrate the range $[b_{min}, b_{max}]$. The mean energy loss of particle 1 (projectile) is thereby given as:

$$-\frac{dE}{dx} = n\int_{b_{\max}}^{b_{\min}} T\, 2\pi b\, db = n\int_{b_{\max}}^{b_{\min}} \frac{Z_1^2 Z_2^2 e^4}{b^2 E}\frac{m_1}{m_2}\, 2\pi b\, db = \frac{2\pi n Z_1^2 Z_2^2 e^4}{E}\frac{m_1}{m_2}\ln\left(\frac{b_{\max}}{b_{\min}}\right)$$

Where the maximal energy transfer T_{max} is an elastic collision between two particles, so by conservation of momentum and energy:

$$T_{\max} = \frac{4m_1 m_2}{(m_1+m_2)^2}E$$

Considering 2 we get:

$$b_{\min} = \frac{Z_1 Z_2 e^2}{2E}(m_1+m_2)$$

For estimating b_{max}, we set the lower bound for energy transfer as the energy required to lift an electron to a higher energy level, we define this as $\Delta E_{min} = I$ being the mean ionization energy. We make this assumption because inelastic collisions have a minimal bound, whereas elastic collisions have spectra that smoothly approach 0, and thereby have a significantly lower probability of having kinetic energy values below I. We define b_{max} as:

$$b_{\max} = \frac{Z_1 Z_2 e^2}{v}\sqrt{\frac{m_1}{m_2 I E}}$$

We therefore derive the mean specific energy loss:

$$-\frac{dE}{dx} = \frac{2\pi n Z_1^2 Z_2^2 e^4}{E}\frac{m_1}{m_2}\ln\left(\frac{4Em_1m_2}{I(m_1+m_2)^2}\right) \tag{3}$$

We've stated a limitation of this model already, but another one is that the focus on electron-alpha interaction in a classically mechanical approach discards other terms such as relativistic corrections and a distant resonant energy transfer term. Considering quantum mechanics, we can evolve 3 into:

$$-\frac{dE}{dx} = \frac{4\pi n Z_1^2 Z_2^2 e^4}{m_2 v^2}\ln\left(\frac{2m_2v^2}{I(1+m_2/m_1)^2}\right) \tag{4}$$

Bethe and Bloch derived a quantum mechanical estimation of the specific energy loss as:

$$-\frac{dE}{dx} = \frac{2\pi z^2 e^4}{E_T}\frac{m_T}{m_e}N_e\ln\left(\frac{4E_T m_e}{Im_T} - K\right) \tag{5}$$

and the stopping cross-section as:

$$\sigma = -\frac{1}{N}\frac{dE}{dx} = \frac{2\pi z^2 e^4}{E_T}\frac{m_T}{m_e}Z\ln\left(\frac{4E_T m_e}{Im_T} - K\right)$$

The Bethe-Bloch formula still suffers from its focus on the electron interaction with alpha particles. At lower energies nuclear stopping increases and, therefore, the result begins to deviate.

So far we've established the interaction of a single projectile particle with a target particle, we can generalise to more complicated atomic structures such as compounds using Bragg's law. We do this by a weighted sum of $\frac{dE}{dx}$ of each individual particle/element. Bragg claims we can assume each contribution to the effective stopping power is independent. The effective parameters of the Bloch-Bethe formula for compounds are summarized as:

$$Z_{\text{eff}} = \sum_i a_i Z_i, \quad M_{\text{eff}} = \sum_i a_i M_i, \quad \ln I_{\text{eff}} = \frac{\sum_i a_i Z_i \ln I_i}{Z_{\text{eff}}}$$

Where a_i is the proportionality factor of each respective component.

Energy Straggling

In the previous part, we focused on the theoretical arguments of the single-interaction events between two particles. Taking a step back, and looking at how multiple alpha-particles interact with a lattice of atoms and mobile electrons, it is clear that individual interactions are hard to observe and are strongly biased by statistical variations[1]. This means meaningful results can only be expressed with a large amount of interactions where values such as, averages, errors and distributions reach constant states and offer themselves to analysis.
The loss in energy ΔE is thus statistically distributed as a normal distribution. The probability density $dW(\Delta E) = f(\Delta E)d(\Delta E)$ is thereby defined as the gaussian density:

$$f(\Delta E)d(\Delta E) = \frac{1}{\Omega_B\sqrt{2\pi}} \exp\left(-\frac{(\Delta E - \langle \Delta E \rangle)^2}{2\Omega_B^2}\right) d(\Delta E)$$

where Ω_B is the standard deviation of ΔE which is also called the Bohr straggling after certain approximations are made. We can rewrite Ω_B as:

$$\Omega_B^2 = \text{Var}[\Delta E] = E[\Delta E^2] - (\langle \Delta E \rangle)^2 \simeq E[\Delta E^2] \tag{6}$$

We can find the expectation of ΔE^2 as:

$$\langle \Delta E^2 \rangle = \int_{\Delta E_{\min}}^{\Delta E_{\max}} \Delta E^2 f(\Delta E) d(\Delta E) = N_e t \int_{\sigma_{\min}}^{\sigma_{\max}} \Delta E^2 d\sigma$$

and the integration term $d\sigma$:

$$d\sigma = \frac{d\sigma/db}{d(\Delta E)/db} d(\Delta E) = -\pi \frac{c}{\Delta E^2} d(\Delta E)$$

giving us the final result, with $N_e = NZ$, $Z_2 = 1$, $m_2 = m \ll m_1$ as:

$$\Omega_B^2 \simeq 4\pi Z_1^2 \epsilon^4 NZt \left(\frac{m_1}{m_1 + m}\right)^2 \simeq 4\pi Z_1^2 \epsilon^4 NZt \tag{7}$$

Note that this is only valid for smaller layers of thickness t. This result tells us that the energy straggling is independent of the initial energy of the projectile and instead depends on the electron density per unit area.
The full width at half maximum $\Gamma = 2\sqrt{2\ln 2}\Omega$ is what we formally define as *energy straggling*. The width Γ of the peak comes from the thickness of the source Γ_Q and the detector resolution Γ_D which are both normally distributed and independent of the interaction Γ:

[1] By statistical variation we mean that random statistical errors are large enough to be worth noting

$$\Gamma = \sqrt{\Gamma_{exp}^2 - \Gamma_Q^2 - \Gamma_D^2}$$

Therefore, we get the energy distribution of the alpha particles as:

$$N(E) = \frac{N_0}{\Omega\sqrt{2\pi}} \exp\left(-\frac{[E - (E_0 - \langle \Delta E_0 \rangle)]^2}{2\Omega_B^2}\right) \tag{8}$$

where N_0 is the total number of particles in the peak and E_0 is the energy before the interaction.

Range

Range is defined as:

$$R(E_0) = \int_0^{E_0} \left(\frac{dE}{dx}\right)^{-1} dE \tag{9}$$

Due to the statistical natuare of the stopping power, the mean range R_m with a range straggling $\Gamma_R = 2\sqrt{2\ln 2}\Omega_R$. We can also use the range to find the initial energy of a known particle. Therefore for our application we use a semi-empirical formula:

$$R(E_0) = R(E_{min}) + \int_{E_{min}}^{E_0} \left(\frac{dE}{dx}\right)^{-1} dE$$

where E_{min} is the minimum valid energy for the Bethe-Bloch formula.
An approximation of the range $R(E)$ is found to be:

$$R(E) = a_2 E^2 + a_1 E + a_0 \tag{10}$$

where the constants a_i are experimentally determined.
The Bragg-Kleemann-rule says that for an identical particle in a different density ρ_i and molar mass M_i we can approximately take:

$$\frac{R_1}{R_2} \approx \frac{\rho_2}{\rho_1}\sqrt{\frac{M_1}{M_2}}$$

As to the range for compounds we can take M_{comp} as the molar mass of the compound and M_i and R_i are the individual components' parameters. a_i is again the relative number of atoms in the compount i.

Experimentally, we find the range and range straggling with the number-distance curve. This defines the count per distance, which means that at different distances between the source and the detector the geometry of the apparatus alters, namely the solid angle. The range spectrum is, up to first order defined by:

$$n(R) = \frac{1}{\sqrt{2\pi\Omega_R^2}} \exp\left(-\frac{(R_m - R)^2}{4\Omega_R^2}\right)$$

where R_m is the mean range, and Ω_R the range straggling.

The fraction of alpha-particles that haven't stopped after penetrating a layer of thickness x is given by:

$$\tilde{n}(x) = 1 - \int_{-\infty}^{x} n(R')dR' = 1 - \int_{-\infty}^{x} \frac{1}{\sqrt{2\pi\Omega_R^2}} \exp\left(-\frac{(R_m - R')^2}{(2\Omega_R)^2}\right) dR'$$

We note that:

$$2(R_{ex} - R_m) = \sqrt{2\pi} \cdot \Omega_{RM}$$

which gives us a definition of Γ_{RM} and thereby the corrected Γ_R is found as:

$$\Gamma_R = \sqrt{\Gamma_{RM}^2 - \Gamma_0^2}$$

With Γ_0 the range straggling at 0 mbar.

Energy loss in foils

There are two methods for calculating the energy loss of an alpha particle passing through an absorber of thickness t.

The first relies on the approximation:

$$\frac{\Delta E}{\Delta x} \approx \left(\frac{dE}{dx}\right)$$

Since we expect $\frac{\Delta E}{\Delta x}$ to be smooth in our range of interest, this linear approximation is close to the behavior of an absorber of thickness $t = \sum_{i=1}^{n} \Delta x_i$ and becomes more accurate the higher n is. Thereby, we've described a numerical integration here:

$$\Delta x_i = \left(\frac{dE}{dx}\right)_i^{-1} \Delta E_i \quad \overset{\Delta x_i \to 0}{\longrightarrow} \quad dx = \left(\frac{dE}{dx}\right)^{-1} dE \tag{11}$$

The second method is simply the integral in 11. Our definition of range 9 can be used to define t:

$$R(E_0) - R(E_t) = \int_0^{E_0} \left(\frac{dE}{dx}\right)^{-1} dE - \int_0^{E_t} \left(\frac{dE}{dx}\right)^{-1} dE = \int_{E_t}^{E_0} \left(\frac{dE}{dx}\right)^{-1} dE = \int_0^t dx = t \tag{12}$$

Experiment

The experiment detects alpha rays in a glass cylinder connected to a vacuum pump. Inside this cylinder, we have our source, detector, and foil revolver[2]. A diagram of this source is found in Figure 2

Our goal is to find the alpha spectrum of the Am-source, find the thickness of several foils, find the stopping range, the straggling range Γ_R, the residual range R_S, the specific energy loss of alpha-particles at different pressures and compare the results with Bohr straggling.
To get the necessary measurements and achieve our experimental goals as efficiently as possible, we take the following procedure:

1. Ensure that the foil revolver is set in the *empty* setting so that we measure the unabsorbed ray.

[2]The foil lets us manually alter the absorber sample between the source and detector without interfering with the isolated system.

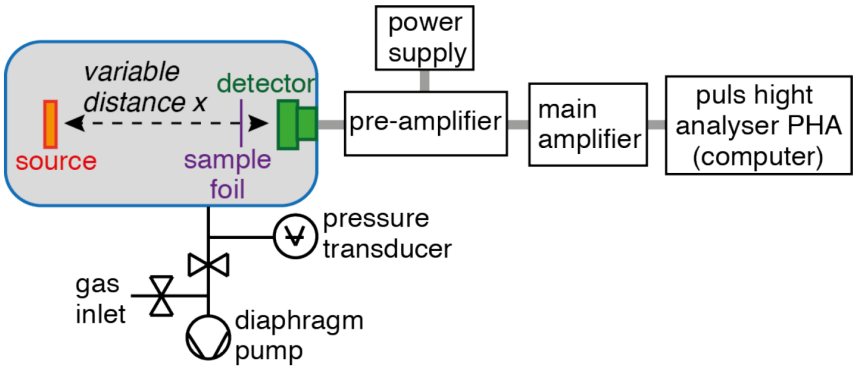

Figure 2: Experimental setup diagram

2. Cover the glass cylinder so that no light can enter the environment and disrupt the detector.
3. Create a vacuum and turn on the detector.
4. Measure the energy spectrum of the alpha source over a fixed time and distance, and this gives us the alpha spectrum of the Am-source. Subsequently, we calibrate according to the values in the literature.
5. In the same vacuum environment, we do the same measurements over different foil samples by rotating the revolver. The spectra are used to find the thicknesses of the respective foils.
6. Still in vacuum, we made measurements of different distances in the range of 38-40mm. This will give us the stopping range, the straggling range Γ_R and the residual range R_S.
7. Now we slowly let in air and increase the pressure of the experimental environment and make measurements to find the energy-pressure relation.
8. Lastly, we turn off the detector before removing the cylinder cover.

Results

Specific Energy Loss of Alpha-particles in Air

We begin with a computation of the Blethe-Bloch-Formula 5 for air. We approximate air as a mixture of Nitrogen N^2, Oxygen O^2 and Argon Ar with relative weights of $a_1 = 0.7847$, $a_2 = 0.2106$ and $a_3 = 0.0047$.[3] The molar masses are taken as $M_1 = 14.01 \cdot 10^-3$ kg/Mol, $M_2 = 16 \cdot 10^-3$ kg/Mol and $M_1 = 39.95 \cdot 10^-3$ kg/Mol. We take the effective relativistic correction $K_{\text{eff}} = 0.650 \pm 0.007$ and the effective mean ionization energy $I_{\text{eff}} = 95.0 \pm 1eV$.[3][2][6][1]
In standard units, we get the result with respective errors in Figure 3. The result in units of [eV/10^{15} atoms/cm^2] and [keV/mm] are found in Figure 4.

[3]We assume only N^2, O^2 and Ar as they are the most abundant in the atmosphere. We also take into account that oxygen and nitrogen are compounds in our relative weights a_i.

Alpha Spectrum of Americium in a Vacuum

For meaningful measurements, we must calibrate our device. For this, we need the energy spectra of a known source. We take the radiation of Americium at a distance of 38mm from the detector and in a vacuum for 2 minutes exactly. The raw data is found in Figure 5.
We note that the raw data contains three discernable peaks which we assume to be the most prevalent excitations of Americium with kinetic energies $5.49 \cdot 10^6$ eV, $5.44 \cdot 10^6$ eV, $5.39 \cdot 10^6$ eV. In order to fit each peak on a Gaussian distribution, we isolate where we expect the strongest peak to be, take the Gaussian (since the other peaks have minimal effect there), and remove this Gaussian from the raw data to get an adjusted data set (Adjustment 1). We do the same process for the next strongest peak until we've identified what we hope are the three highest probability-weighted kinetic energies.

We get the summary of attributes for each peak in Table 1.

Parameter	**Peak 1**	**Peak 2**	**Peak 3**
Kinetic Energy (eV)	$5.486 \cdot 10^6$	$5.443 \cdot 10^6$	$5.388 \cdot 10^6$
Peak Position (eV)	$7.658 \cdot 10^6$	$7.604 \cdot 10^6$	$7.528 \cdot 10^6$
Peak Width (eV)	$4.531 \cdot 10^4$	$5.078 \cdot 10^4$	$7.543 \cdot 10^4$
Peak Height	265.7	73.05	12.14
Peak Volume (eV)	$1.204 \cdot 10^7$	$3.709 \cdot 10^6$	$9.157 \cdot 10^5$
Abundance	0.7225	0.2226	0.05494

Table 1: Attributes of our Measured Peaks

Then we calibrate to get Figure 6 with the result for a linear fit $f(x) = mx + c$ as $m = 1.39672 \pm 0.00069$ and $c = 0.052 \pm 3.257$ keV.

Thickness of Foils

We find the energy distributions of the different foils in Figure 7.

Then, we use the first method 11 to perform a numerical integration where the range is approximated by a polynomial 10. Subsequently, we use the 12 that integrates with the Bethe-Bloch formula. The results are summarized in Table 2. The constants and their errors used in these calculations are found in the manual.[6]

Name	Al-2	Al-3	Au-7	Co-5	Cu-4	Mylar-8
Polynomial Thickness (µm)	26.2	0.0456	5.94	5.91	20.2	54.0
Polynomial Error (µm)	1.60	0.524	0.578	0.305	2.37	1.97
Bethe-Bloch Thickness (µm)	26.4	0.0578	5.90	5.74	20.4	-
Bethe-Bloch Error (µm)	1.53	0.519	0.565	0.287	2.34	-

Table 2: Thickness of respective element samples of both methods 11 and 12.

Counts per Distance in Air to find the Stopping Range

Figure 8 summarized our results nicely. We found the mean range R_m = and the extrapolated range as R_{ex}. For this we had to use the SRIM simulation[7] to find the residual range:

$$R_S = \frac{3}{2} \frac{E_S}{-(dE/dx)_S} = 1.66 \cdot 10^{-3} m \tag{13}$$

and adding it to our data. We also found the straggling to be $9.56 \cdot 10^{-4} m$

Specific Energy Loss over varying Pressures

We find the energy readings for different pressures in Figure 9 which give us the effective layer thickness relation to energy given in 10 using the formula $x = x_0 \frac{p}{p_0} \frac{T_0}{T}$ with $p_0 = 1013.25$ hPa, $T = 296.15$ K and $T_0 = 273.15$ K.[6]

Then, taking the negative derivative of 10 give us Figure 11 and the Bragg curve on Figure 12. From this we find the maximum energy loss 459 MeV/m and the respective energy at that point being 1.6 MeV and the position 32 mm.

We then consider the Straggling of the Am-source, so Ω_B, the comparison of this with the theoretical value 7 is given in Figure 13. Then, if we adjust for the experimental Γ_{exp} that we obtain for the alpha source in a vacuum, we get the comparison of the theoretical and experimental Full-Width-Half-Maximum in Figure 14.

Discussion

Our first result is purely computational. The calculation of the specific energy loss of alpha-particles in air let us see how we theoretically expect the energy-stopping power relation to look like; additionally, we see that results in low energy become unreliable and approach a singularity.
We already expected this from our theoretical excursion of the Bethe-Bloch formula 5, but from Figure 3 we can already see that the positional derivative of energy tends towards $-\infty$ which physically translates to: very small energy levels gain a lot of energy from the absorption in air, violating energy conservation laws.[4] A mathematical analysis using domination laws on 5 also confirms this fallacy without any computation.

Our first experimental results for calibration as summarized in Table 1 are not direct measurements, but were found by certain manipulations and data extractions as visualized in 5.
A key problem for our calibration was that the resolution was too poor for a Gaussian fit on one the peaks to not be heavily influenced by the other peak. Therefore, as a solution, we took a Gaussian fit on an isolated part of the highest peak where the influence from the other peaks was minimum. The removal of this Gaussian trend from the raw data gives us an adjusted set of peaks that are not influenced by the dominant (highest) peak. We then do the same to the next highest peak until the adjusted data is more or less flat, as seen with the pink line (*Adjustment 3*). By this method, we were able to find three prominent peaks that matched the kinetic energy of the three highest probability excitations of the americium source. Other notable attributes of the Gaussian fits is that the show relatively good standard deviations of about 1% relative to the energies.
Table 1 gives us our calibrations: Figure 6. The error of the one-point fit is relatively low, for the gradient it is $m = 1.39672 \pm 0.00069$ and $c = 0.052 \pm 3.257$ keV. A key improvement would be to find a source that would give us calibration values in the lower energy range, this would make the y-intercept c closer to 0 with a much smaller error than what we have.

Now we consider the thickness of our sample foils made of elements Aluminum, Gold, Cobalt, and Copper. Table 2 summarizes these results using the two methods mentioned in the theory. We note that in general the results coincide in the first significant figure almost consistently, the exception being Al-3 which is justified later. The errors are also quite similar in magnitude and sit at about 10% relative error, which makes it rather

[4]The violation of energy conservation is supported by the order of the energy gain with respect to the energy, 1 electron volt can support an energy gain significantly higher than the order of 10.

imprecise. Despite this, one can note that the different methods have results that sit within their respective standard deviation, which solidifies the validity of the theoretical background.
Al-3 seems to be an outlier to the rest of the results, it's high error relative to the result and its absurdly low thickness implies that the sample foil there is most likely damaged. This might have happened due to rapid pressure changes in the cylindrical chamber causing the foil to break, or perhaps it was set up like this by the supervisors to confirm our results are reasonable (this would also perhaps explain why there are two aluminum samples).

The results shown in Figure 8 has a uniform structure that gives us the expected results. We are able to make a nice Gaussian fit and find the maximal stopping within a close range to our literature values.
An improvement would be to consider calculating more data points within the range of the strong change (36.5mm - 38.5mm). This would give us a more accurate fit.

Finally, the specific energy loss over varying pressures gives us an interesting alternative approach to the previous measurements. We identify pressure with distance and define how the energy of the peak varies. This allows us to model the energy loss over distance and the Bragg curve as seen in Figures 11 and 12. A key results shows that the maximum energy loss is found 32mm, since this is the last result of an increasing energy loss, it is expected that the actual maximal loss could be even further away. The only way we could've extended our range if we were to have a better vacuum engine or something that could increase the air pressure in the casing higher than what was in the room at that time.
Despite this, the results seemed to follow a particular curve quite continuously and the error is relatively low.
Looking towards the Bohr straggling, we see that the variance relation between the theoretical and expected values is quite large. If we make the adjustment for the straggling by removing the error due to the experimental setup, Γ_{exp} we see less distance between the experimental and theoretical curve, but still quite a large difference.
This could potentially be attributed to anomalous energy straggling, the cause of which comes from the energy dependence of the specific energy loss. The Bragg curve establishes that higher energy readings have a lower energy loss and smaller peak width, independent of the Bohr Straggling. There is then a monotonic increase as energy decreases, which explains why the experimental gamma not only does not match the theoretical values too well, but also stray away from them as position increases.
The higher the energy loss effect, the less accurate is the Bohr approximation, as quantified in the last two figures. A possible improvement to this experiment is to, therefore, record where energy loss is minimized, which means more precise tools and equipment, but still the relative error is expected to be large.

Conclusion

In conclusion, of our three main tasks, we could complete two of them with a satisfying enough conclusion. The measurement of the foil thickness of the different samples showed consistent results in view of two different theoretical and computational approaches. Despite the error being relatively high, it is more convincing than our other results.
The stopping range gave us satisfying results consistent with the expected behaviour of the activity source over different distances near the threshold.
The specific energy loss due to the pressure changes, on the other hand, proves to have more convincing results in that we have at least a curve-like behaviour of our data

points (in other words, there are no sharp Brownian-like oscillations as seen in Figure 8) but when comparing with the Bohr straggling we still see a great difference in what we expect from what we get. We could, at least, potentially attribute this towards a particular cause, namely anomalous energy straggling, but I personally doubt it should have so strong an effect as we see.
Overall, there seems to be indications that things did mostly go as expected, but as to the final results, they lack the precision needed to make scientific conclusions on the phenomena we modelled. A more precise approach to measurement is needed, as well as perhaps a more complex theoretical dissection.

Appendix

This report benefitted from ChatGPT and DeepSeek for LaTeX table formatting and python syntax recollection. However, it was not used to write text or code.

References

[1] Wikipedia.
Density of Air.
`https://en.wikipedia.org/wiki/Density_of_air`

[2] PTable.
Dynamic Periodic Table.
`https://ptable.com/?lang=en#Properties`

[3] Wikipedia.
Atmosphere of Earth.
`https://en.wikipedia.org/wiki/Atmosphere_of_Earth`

[4] Wikipedia.
Alpha Particle.
`https://en.wikipedia.org/wiki/Alpha_particle`

[5] Wikipedia.
Impact Parameter.
`https://en.wikipedia.org/wiki/Impact_parameter`

[6] ETH Zurich.
Alpha Absorption Measurement Manual.
`https://p3p4.phys.ethz.ch/manuals/Alphaabsorption_Nov_2013.pdf`

[7] SRIM (Stopping and Range of Ions in Matter).
SRIM-2013.00 Software and Database.
`http://www.srim.org`

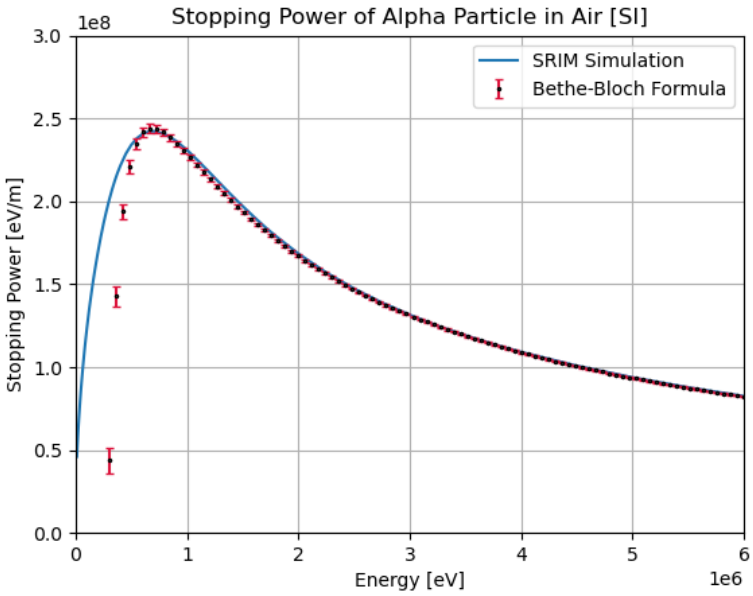

Figure 3: Specific Energy loss in Air According to the Blethe-Bloch-Formula and SRIM simulation [7]

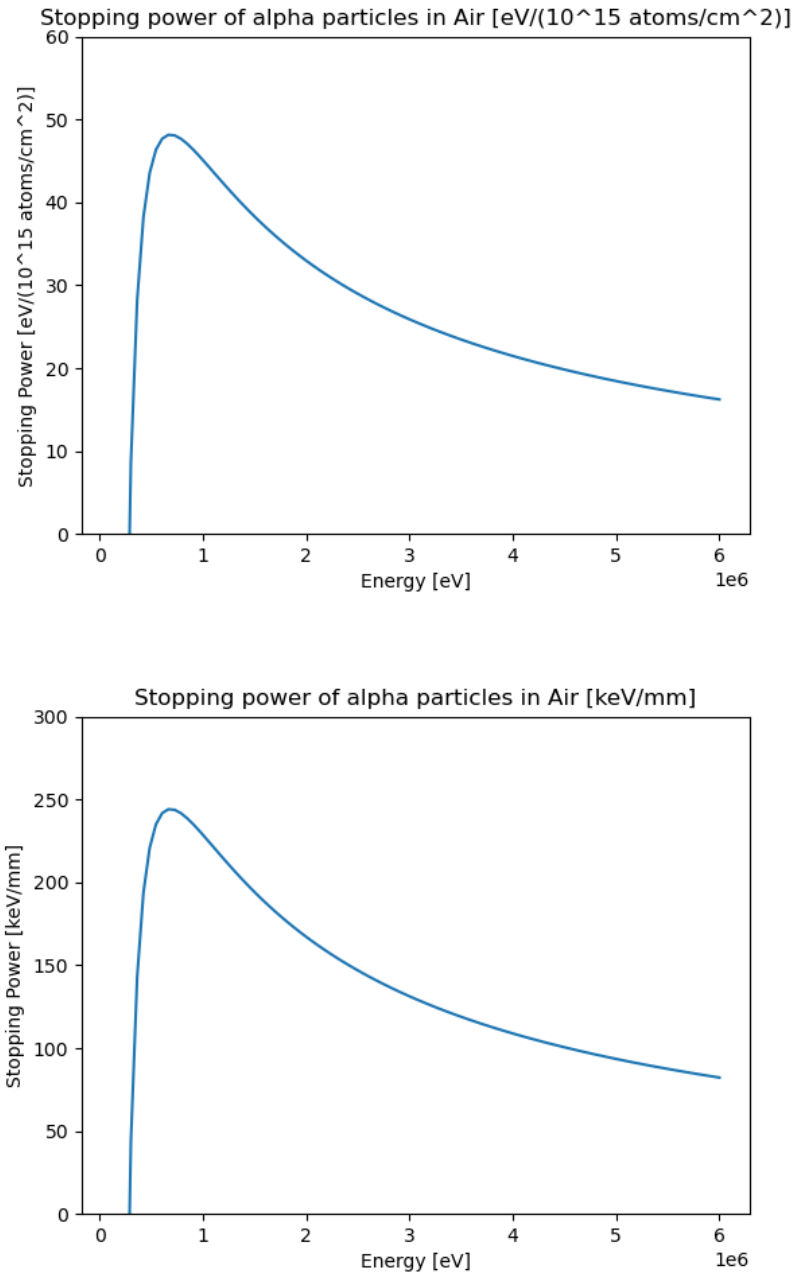

Figure 4: Specific Energy loss in Air in units of [eV/10^{15} atoms/cm^2] and [keV/mm] respectively.

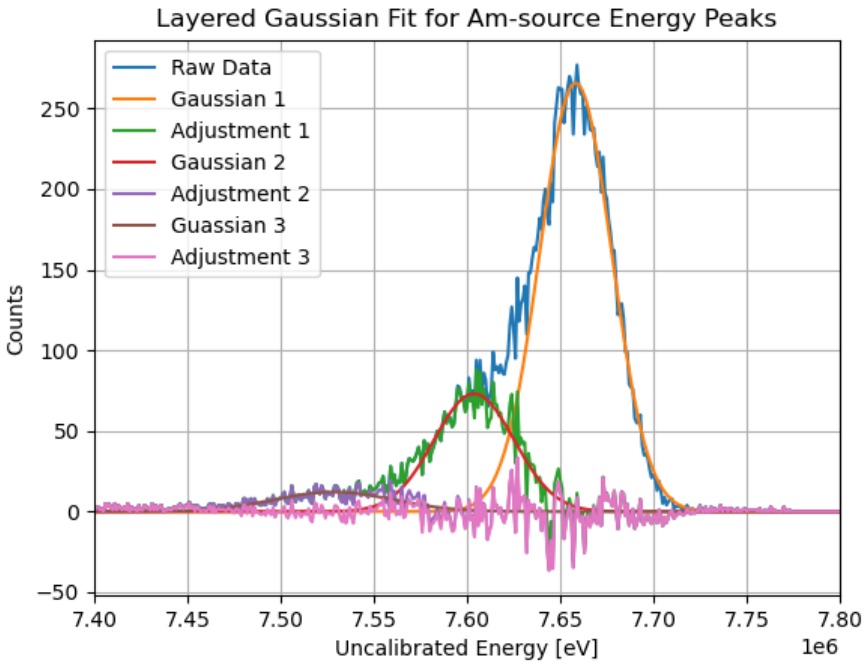

Figure 5: Alpha spectrum of Americium with Gaussian adjustments for Calibration

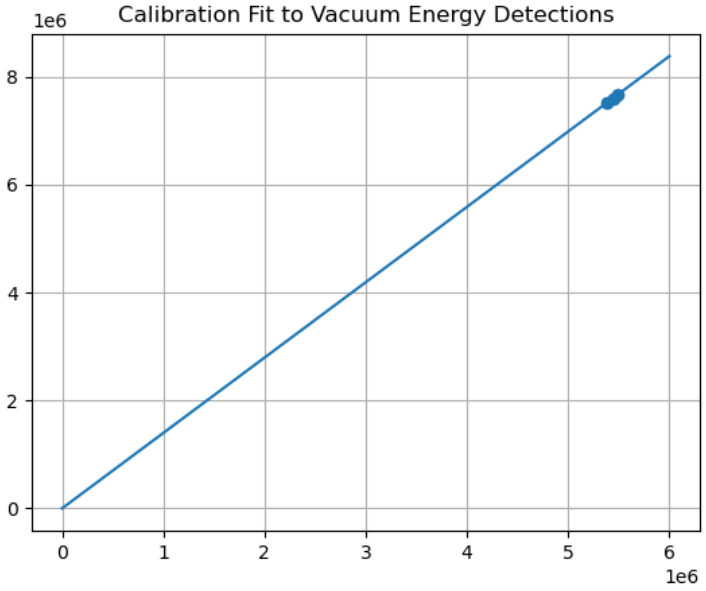

Figure 6: Calibration curve do to the results of Figure 5 with literature values of the kinetic energy

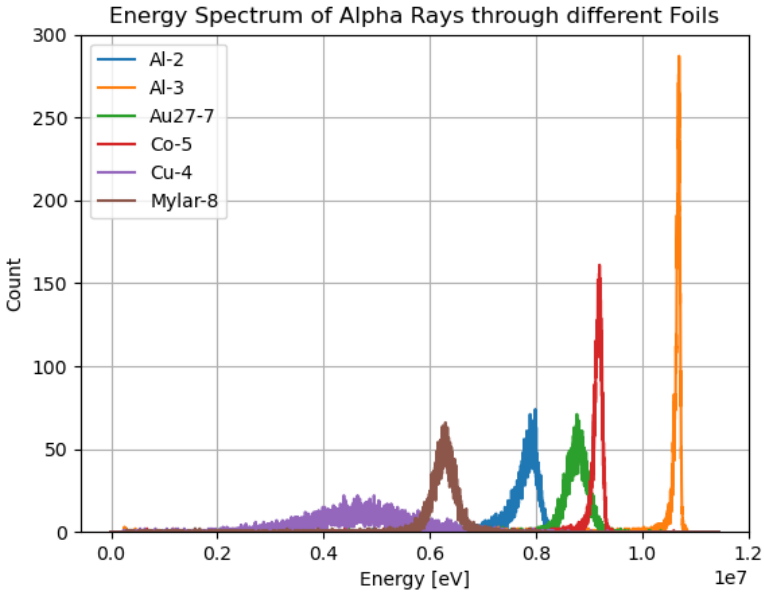

Figure 7: Energy Spectrum of Alpha rays through two aluminium samples, a gold sample, a cobalt sample, a copper sample and a Mylar sample.

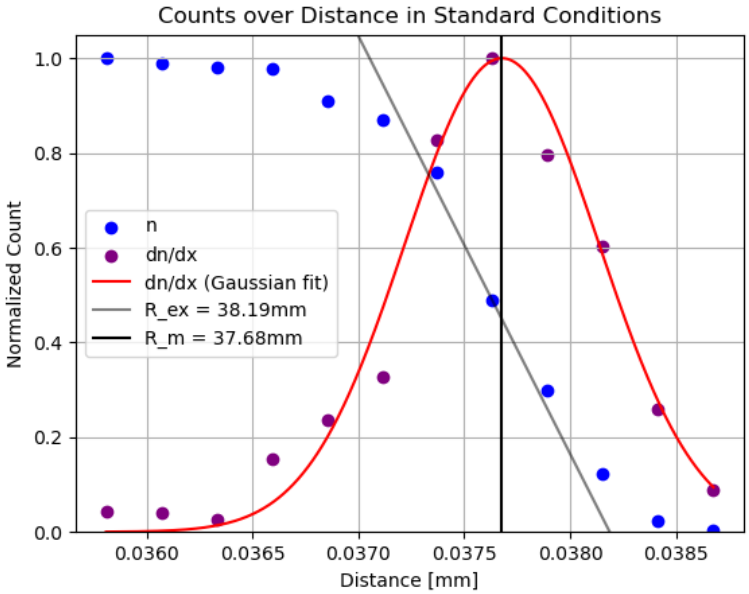

Figure 8: The normalized count over distance (scaled for the solid angle) of an alpha emission in air.

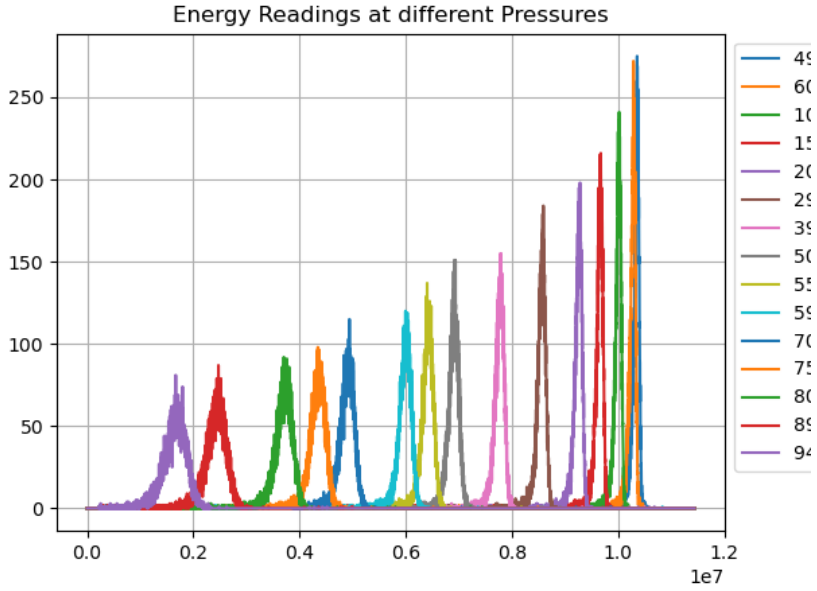

Figure 9: Energy spectra of an alpha emission over different pressures

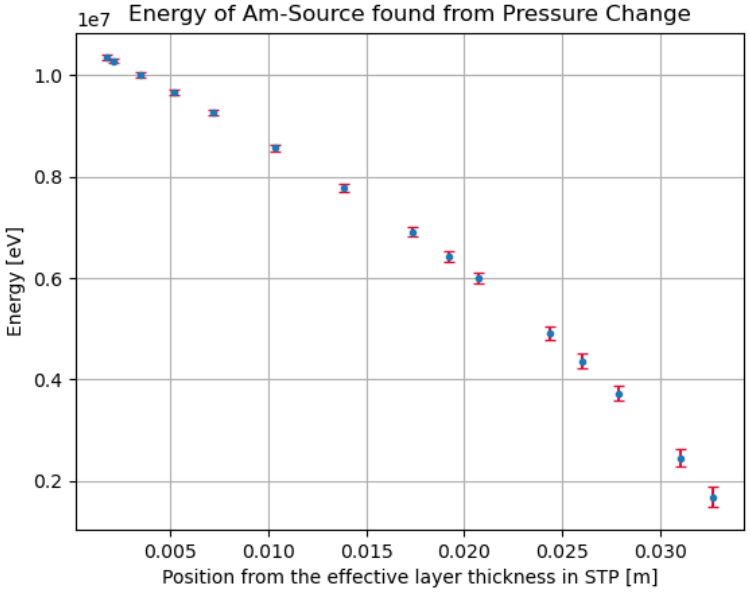

Figure 10: Energy of Am-source with respect to pressure change [Pa] which is transformed into the effective layer thickness [m].

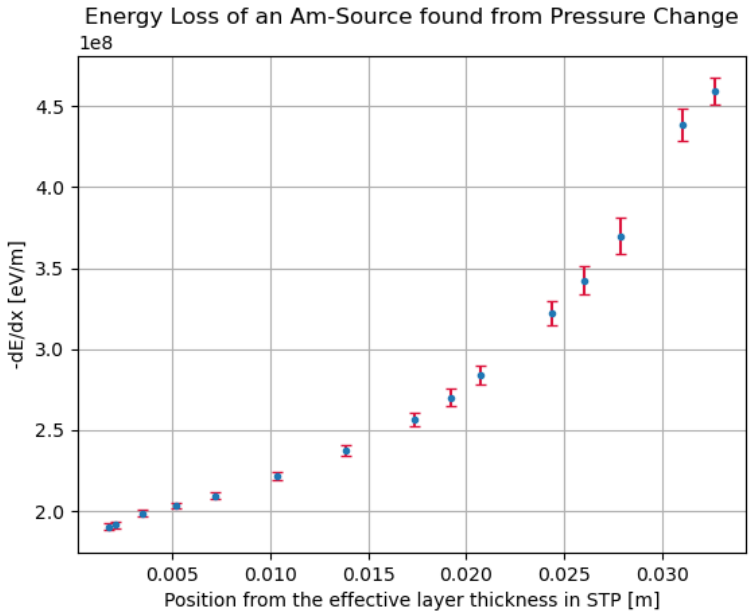

Figure 11: Energy loss of an Am-source with varying pressure.

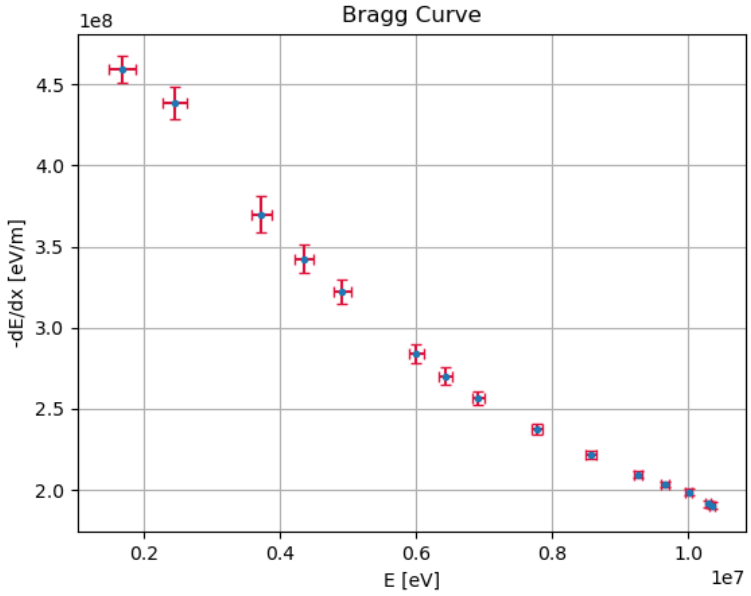

Figure 12: Bragg curve estimation, giving us the loss of energy over energy.

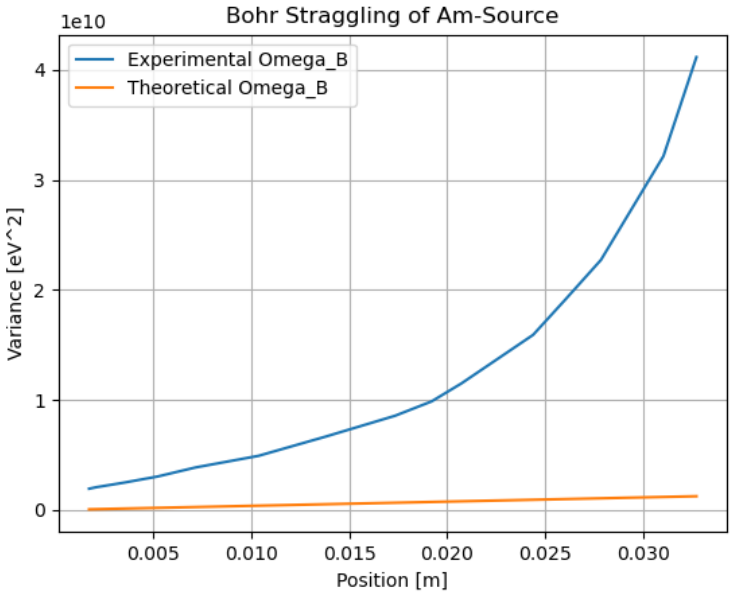

Figure 13: Experimental variance per position against the expected theoretical Bohr straggling.

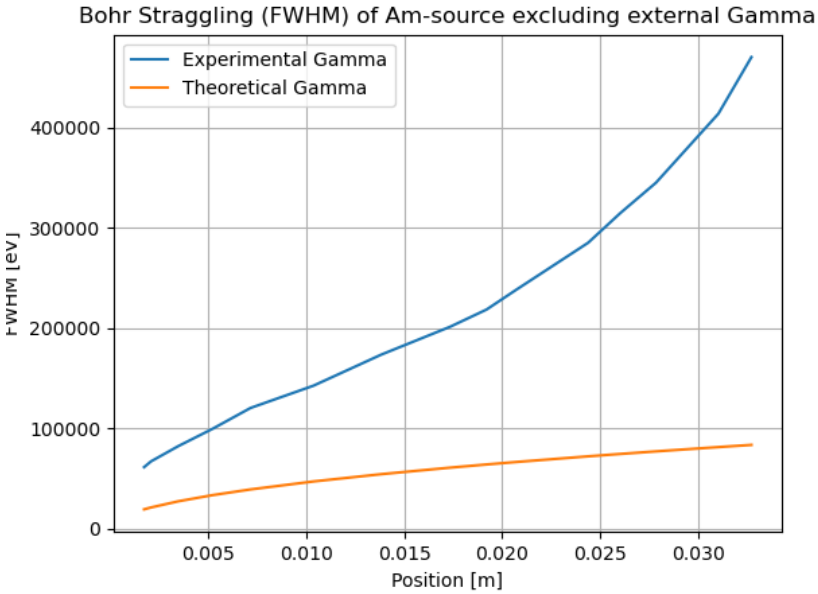

Figure 14: Experimental FWHM per position against the expected theoretical Bohr straggling FWHM.